



ELSEVIER

International Journal of Mass Spectrometry 179/180 (1998) 309–317



Ion bombardment of PbO₂ films: water influence of cluster production

R. Amadelli^a, A.B. Velichenko^b, E. Tondello^c, L. Armelao^c,
S. Daolio^{d,*}, M. Fabrizio^d

^aCentro di Studio Fotoreattività e Catalisi, C.N.R., Dipart. Chim. Univ. Ferrara - via Borsari 46-Ferrara, Italy

^bDep. Phys. Chem., Ukrainian State Chem. Techn. Univ., Gagarin Avenue, 8-Dnepropetrovsk 320005, Ukraine

^cDipart. Chimica Inorg, Metallorg. Analitica, Università di Padova, via P. Loredan 4 - 35131 Padova, Italy

^dIstituto di Polarografia ed Elettrochimica Preparativa C.N.R., Corso Stati Uniti 4, 35127 Padova, Italy

Received 18 May 1998; accepted 30 July 1998

Abstract

Secondary ionization mass spectrometry experiments were carried out in order to study the influence of water on modification of mass spectra obtained from Pb oxide films submitted to aging, heating, and electrochemical treatments. Significant information was obtained about the effect of water on the production of homo- and heterometal clusters and their ionic yields. Interesting aspects have been observed on films electrodeposited from either alkaline or acidic baths. Radiochemical experiments involving measurements of β -activity as a function of deposition temperature and film thickness confirmed the presence of water in the film bulk. (Int J Mass Spectrom 179/180 (1998) 309–317) © 1998 Elsevier Science B.V.

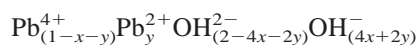
Keywords: Pb oxides; Surface techniques; SIMS; Radiochemical activity; Water–Pb oxide interaction

1. Introduction

It is well known that PbO₂ exists in two different allotropic forms (α and β) both of which deviate from ideal stoichiometry. These deviations are more pronounced for the electrochemically prepared oxide than for chemically obtained samples, and especially more for the α -PbO₂ than the β -PbO₂ form.

It is now widely held that the reason of this nonstoichiometry is the presence of lead vacancies in the crystallographic structure. In the model recently

proposed by Ruetschi [1,2] these vacancies are arranged to form layers (named “internal surfaces”) between crystallographically ordered areas, and the charge of each missing Pb⁴⁺ ion is compensated for by either only OH⁻ ions or by both Pb²⁺ and OH⁻. Thus, the following formula has been proposed as better describing the composition of PbO₂:



This model accounts for the fact that experimental studies report evidence for the presence of Pb(II) [3] and structural water [4–13] in the PbO₂ lattice. These studies generally recognize that there is proportionality between its hydrogen content and its electrochem-

*Corresponding author.

Dedicated to Professor Fulvio Cacace in recognition of his outstanding contributions for many decades to gas-phase ion chemistry and physics.

Table 1
Positive cluster ions

m/z	Ion	Ti/PbO ₂ as prepared	Ti/PbO ₂ heated	Ti/PbO ₂ aged	Ti/PbO ₂ polarized
208	Pb	●●●	●●	●●●	●●●●
224	PbO	●●	●	●●	●●
225	PbOH	●	●		●●
231	PbNa	●●	●●	●●	●●
247	PbNaO	●●●●	●●●●	●●●●	●●●●
254	PbNa ₂	●			●
263	PbNaO ₂	●			●●●
270	PbNa ₂ O	●●	●●		
280	PbNaO ₃	●			●●
286	PbNa ₂ O ₂	●●	●		
309	PbNa ₃ O ₂	●	●●		
325	PbNa ₃ O ₃	●●			
414	Pb ₂	●			●●
430	Pb ₂ O	●●	●●		●●●
446	Pb ₂ O ₂	●	●		●●
469	Pb ₂ NaO ₂	●●	●		●
485	Pb ₂ NaO ₃				●●
492	Pb ₂ Na ₂ O ₂	●●			
508	Pb ₂ Na ₂ O ₃	●			
531	Pb ₂ Na ₃ O ₃	●			
654	Pb ₃ O ₂	●●			
668	Pb ₃ Na ₂	●			
670	Pb ₃ O ₃	●			
691, 693	Pb ₃ NaO ₃ , Pb ₃ Na ₃	●			
716	Pb ₃ Na ₂ O ₃	●			

●●●● indicate the most intense peaks for m/z range > 200.

●●● intensity \geq 5% than ●●●●.

●● intensity \geq 1% than ●●●●.

● intensity < 1% than ●●●●.

ical activity. It seems, however, that there has been insufficient systematic investigation as to how the control of the different parameters in the electrodeposition of PbO₂ can affect the amount of structural water in the resulting oxide. The effect of subsequent treatments following electrodeposition, such as heating, would also merit further study. It is known, for example, those heat-treated electrodes are more active in the production of O₃ at high potential [14].

Previous secondary ion mass spectrometry (SIMS) studies carried out in the laboratory on PbO₂ films [15–17] showed the potential of the technique in providing information from both positive and negative ion species detected as a result of different electrosynthesis conditions.

The present article describes the results of SIMS investigations on β -PbO₂ obtained by electrodeposi-

tion either from basic or acid solutions. The aim is to contribute to the understanding of the presence of structural water at the surface and in the bulk oxide and of its influence on the distribution and reactivity of alkaline metal bath components. SIMS and radiochemical data will be presented evidencing the incorporation and distribution of protons in PbO₂ films electrodeposited either from ²H₂O or ³H₂O.

2. Experimental

All chemicals were Fluka (Milano, Italy) products, deuterated water was obtained from Aldrich Chimica (Milano, Italy). Ti cylinders 1 cm in diameter and 0.5 cm thick were used to prepare electrodic films. The cylinders were etched in a 20% oxalic acid solution at 80 °C for periods ranging from 10 to 20 min.

Table 2
Negative cluster ions

<i>m/z</i>	Ion	Ti/PbO ₂ as prepared	Ti/PbO ₂ heated	Ti/PbO ₂ aged	Ti/PbO ₂ polarized
208	Pb	●●	●	●●	●●
220	PbC	●	●	●	●●
224	PbO	●●●	●●	●●	●●
225	PbOH	●	●	●	●
226	PbOC	●	●	●	●
240	PbO ₂	●●●●	●●●●	●●●●	●●●●
241	PbO ₂ H	●	●	●	●
242	PbO ₂ H ₂				
247	PbNaO	●			●
256	PbO ₃	●●	●		●●
257	PbO ₃ H	●	●		●
258	PbO ₃ H ₂				●
263	PbNaO ₂	●●	●	●	●
279	PbNaO ₃	●			●
280	PbNaO ₃ H	●			●
295	PbNaO ₄	●			●
302	PbNa ₂ O ₃	●			●
414	Pb ₂	●			●
430	Pb ₂ O	●	●	●	●
446	Pb ₂ O ₂	●	●		●
462	Pb ₂ O ₃	●●	●	●	●●
485	Pb ₂ NaO ₃	●			●
670	Pb ₃ O ₃	●			
686	Pb ₃ O ₄	●			●
707	Pb ₃ NaO ₄	●			

●●●● indicate the most intense peaks for *m/z* range > 200.

●●●● intensity ≥ 5% than ●●●●.

●●●● intensity ≥ 1% than ●●●●.

●●●● intensity < 1% than ●●●●.

The β -PbO₂ samples for SIMS measurements were prepared by electrodeposition either from Pb(NO₃)₂ basic (1 M NaOH) or acidic (1 M HNO₃) solutions. The PbO₂ deposits were obtained under galvanostatic conditions at 5 (basic bath) or 10 mA cm⁻² (acidic bath) constant current supplied by an Amel potentiostat/galvanostat Model 553 (Amel, Milan, Italy).

The influence of the different treatments was studied on four β -PbO₂ coating groups electrodeposited from basic solutions. Group A was analyzed as prepared; group B after natural aging (1 year); group C after heating at 60 °C for 24 h; group D after electrochemical treatment (10 voltammetric cycles at 5 mV s⁻¹ from -0.3 to 1.2 versus Ag/AgCl in 1 M HClO₄ solution at pH 11).

Isotopic exchange experiments were carried out on β -PbO₂ coatings electrodeposited from an acidic bath

at room temperature. β -PbO₂ films underwent different processing; samples E were obtained in acidic H₂O, samples F in acidic ²H₂O and samples G in acidic ²H₂O and then dipped for 48 h in acidic H₂O.

Several radiochemical measurements were carried out on α -PbO₂ and β -PbO₂ samples prepared from ³H₂O-enriched solutions. α -PbO₂ was electrodeposited at 23 °C, while β -PbO₂ was synthesized at 23 and 60 °C, respectively, as described in the literature [18]. Once the desired layer thickness was achieved, the deposit was dissolved in aqueous solutions of acetic acid containing H₂O₂. Aliquots of these solutions were added to an Insta-Gel Packard (Canberra, Australia) scintillation liquid and the activity counted using a beta TriCarb 300C Packard (Canberra, Australia) equipment.

SIMS measurements were carried out in a custom-

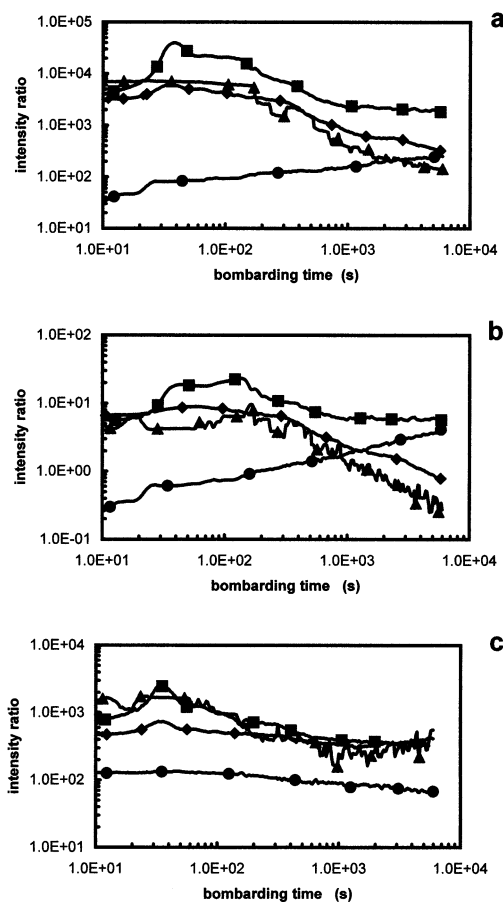


Fig. 1. Intensity ratio (a) Na^+/Pb^+ ; (b) $\text{PbNaO}^+/\text{Pb}^+$; (c) $\text{Na}^+/\text{PbNaO}^+$ for as prepared (filled square); heated (filled diamond); aged (filled triangle); polarized $\beta\text{-PbO}_2$ coatings (filled circle).

built instrument described elsewhere [19]. A monochromatic 10 keV O_2^+ ion beam (collimated to 50 μm) was generated in a mass-filtered duoplasmatron ion gun. Sputtered species were collected in a Balzer QMA 400 quadrupole mass analyzer. Sputtering rate was evaluated between 80 and 200 nm/min with an ionic current range between 400 and 800 nA.

3. Results and discussion

Different experiments of $\beta\text{-PbO}_2$ electrodeposition from basic solution gave films of varying thickness, from 26 to 34 μm , confirming the choice of synthesis conditions. The positive ion mass spectra obtained

from different areas of the samples show reproducible data. In the low mass range, peaks that originated from the presence of organics ($m/z = 12, 13, 14, 15$), oxygen ($m/z = 16, 32$), alkaline metals ($m/z = 7, 23, 39$), and other minor impurities were evidenced. In particular, in addition to Na^+ ions that correspond to the base peak of the spectra, NaO^+ ($m/z = 39$), Na_2^+ ($m/z = 46$), Na_2O^+ ($m/z = 62$), Na_2OH^+ ($m/z = 63$), Na_3^+ ($m/z = 69$), Na_2O_2^+ ($m/z = 78$), Na_3O^+ ($m/z = 85$), Na_3O_2^+ ($m/z = 101$), $\text{Na}_3\text{O}_3\text{C}^+$ ($m/z = 129$) are all present in significant ion abundance. It is pertinent to examine their role in the film properties carefully. In fact, the high reactivity between alkaline metal and Pb oxide in as prepared samples also strongly influence the ion species production in the higher mass range of the spectra.

From Table 1 it is evident that most of the peaks are due to $\text{Pb}_x\text{Na}_y\text{O}_z^+$ ($x = 1-3, y = 1-3, z = 0-3$) heterometal clusters and the PbNaO^+ species is characterized by the higher ion yields. Many other heterometal clusters showing good ion intensities are of interest and in different experiments their origin seems to be affected by alkaline metal and water or hydroxyl species distribution.

In order to evaluate a possible correlation between water presence and mass spectra modification, the four series of $\beta\text{-PbO}_2$ films from alkaline solutions were bombarded with O_2^+ primary ions at the same energy. Drastic modifications of spectra were detected, leading to the following considerations:

In every spectrum, Na^+ ions correspond to the

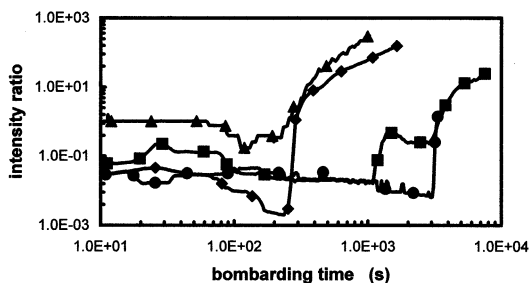


Fig. 2. Ti^+/Pb^+ intensity ratio as a function of bombarding time for as prepared (filled square); heated (filled diamond); aged (filled triangle); polarized $\beta\text{-PbO}_2$ coatings (filled circle).

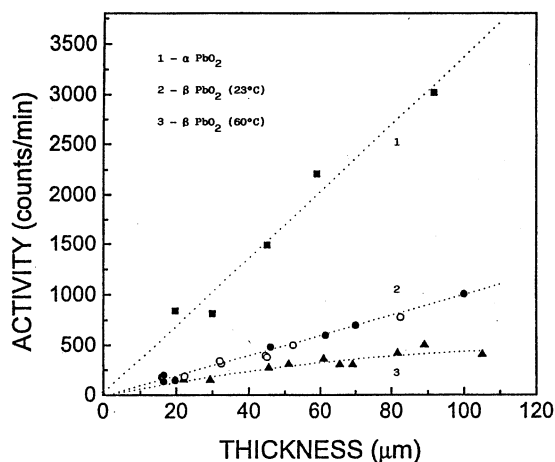


Fig. 3. Tritium activity of PbO_2 deposits as a function of thickness and, for $\beta\text{-PbO}_2$, electro-synthesis temperature.

base peak but the homo- and heterometal cluster ion yields are strongly reduced: Their relative abundance decreases when samples are heated at 60°C (under vacuum conditions for 1 h), and decreases again if samples are aged for 1 y.

The aged film shows only PbNa^+ and PbNaO^+ heterometal cluster ions and in particular the $\text{PbNaO}^+/\text{Pb}^+$ ion intensity ratio is strongly reduced.

The $\text{PbNaO}^+/\text{Pb}^+$ ion intensity ratio decreases again in the polarized film and Pb^+ becomes the highest PbO_2 -related peak.

The sample polarization causes an increase in the relative abundance of many cluster ion species; heterometal cluster ions containing more than two sodium atoms are absent, while the observed heterometal cluster ions contain only one sodium atom.

OH^+ signals are higher in the untreated and polarized samples while PbOH^+ are absent in the heated and aged films.

The negative ion mass spectra also give a rich picture of very interesting peaks: O^- ions correspond to the base peak and many hydroxide, homometal and heterometal cluster ion species are present. In particular in the low mass range the peaks of organic fragments, O^- , OH^- , O_2^- , Cl^- are predominant while in the mass range >200 units the numerous ion species shown in Table 2 have been identified and PbO_2^- ion species exhibit the highest ion abundance.

It can be observed that Pb_xO_y^- ($x = 1-3$, $y = 1-4$) predominate over $\text{Pb}_x\text{NaO}_y^-$ ($x = 1-3$, $y = 1-4$) ion species; in the heated and aged samples their ion yields are strongly reduced and increase again in the polarized samples. Analogous considerations can be done for hydroxide ion species (OH^- , PbOH^- , PbO_2H^- , PbO_3H^- , and PbNaO_3H^-) that give less intense peaks for heated and aged samples.

Many significant signals have been followed during primary ion bombardment in order to evaluate the in-depth modifications induced by the different tests and Fig. 1 gives Na^+/Pb^+ and $\text{PbNaO}^+/\text{Pb}^+$ ion intensity profile ratios. The curves [Figs. 1(a) and 1(b)] of untreated $\beta\text{-PbO}_2$ films increase after 2–3 min of bombardment, maintain high values for about 3 min and decrease again in the inner layers. Heating and aging tests induce the disappearance of the curve maximum, after attaining a fairly constant value for about 5 min it decreases immediately. On the contrary surface values of polarized samples are very low and increase continuously on in-depth bombardment. These data confirm that strong modifications were induced not only on the surface region (as evidenced by mass spectra), but also in the deepest layers. Na^+/Pb^+ and $\text{PbNaO}^+/\text{Pb}^+$ ratios reach a value comparable to that of other samples after a long bombardment time, while $\text{Na}^+/\text{PbNaO}^+$ ratios [Fig. 1(c)] maintain a quite similar and constant value for nonpolarized films. In fact, the electrochemical test changes the heterometal cluster ion yield. Also in the case of a high Na^+/Pb^+ ratio, the $\text{Na}^+/\text{PbNaO}^+$ value is about one order of magnitude less than in the other cases.

Interesting aspects, concerning the water content, can be emphasized by Ti^+/Pb^+ ion intensity profile ratios: Fig. 2 shows that Ti support signals increase after 300–400 s of bombardment for heated or aged films and more than 1000 s for the untreated and polarized films. Pb oxide thickness was reduced drastically by water loss and its recovery became possible by electrochemical treatments.

Information obtained from the analyses of OH^- , PbO_2^- , Pb_2O_3^- , TiO_3^- , $\text{Pb}_2\text{NaO}_3^-$ signals are absolutely in agreement with those achieved by means of positive ion profiles, while potential new aspects resulted

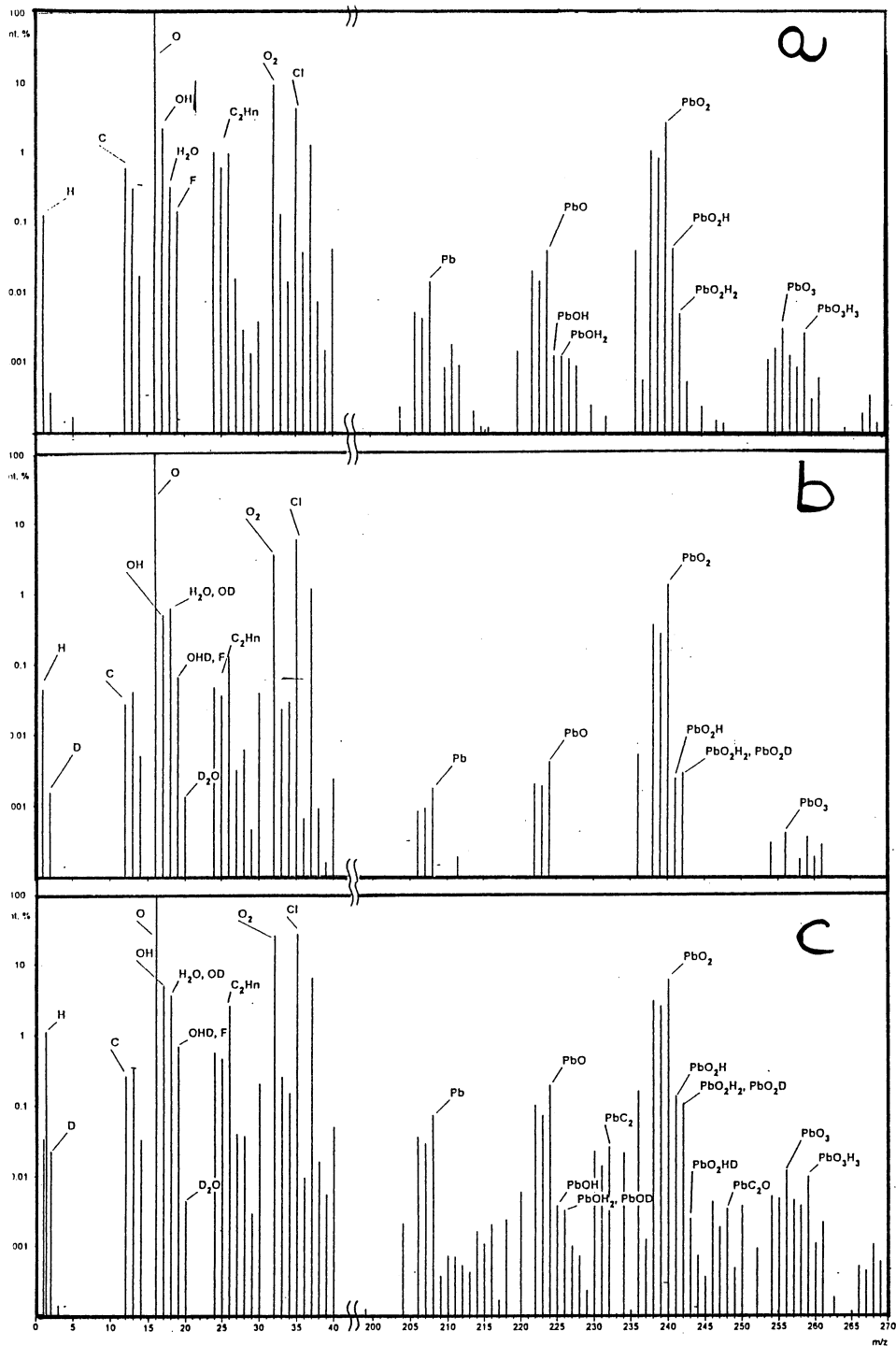


Fig. 4. Negative ion mass spectra recorded for samples from group (a) E, (b) F, and (c) G.

from a different series of investigations on Pb oxide films electrodeposited from $^2\text{H}_2\text{O}$, $^3\text{H}_2\text{O}$ or H_2O acid solutions.

The dependence of water content from film thickness was verified by some radiochemical experiments as shown in Fig. 3 by the uptake of tritium into PbO_2 . The linear dependence of β^- activity from coating thickness confirms the penetration of water along the oxides. In particular, the results indicate that the water amounts incorporated into the coating strongly depend on the allotropic form of the oxide, on the temperature of deposition and, more generally, on the synthesis procedures.

With the aim of obtaining information about water distribution in the electrodeposited films, some experiments with $^2\text{H}_2\text{O}$ were designed and the potential of SIMS in the detection of isotope patterns was used in order to compare data obtained from samples E, F, G containing different amounts of deuterium. The positive ions originating from all samples are qualitatively similar and besides the expected signals of Pb^+ and PbO^+ species, intense peaks related to impurities (Na^+ , K^+ , Si_xO_y^+ , organics, etc.) and to support material (Ti^+ , TiO^+) are present.

On the contrary, significant differences have been obtained from negative ion mass spectra. Other than impurities and support peaks, interesting ion species have been originated with good ion yields and, in particular, the in-depth profile modification related to HO^- ($m/z = 17$), $^2\text{HO}^-$ ($m/z = 18$), H_2O^- , H^2HO^- , $^2\text{H}_2\text{O}^-$ seems to be able to evidence water distribution in the different samples. Fig. 4(a) shows PbO_3H_3^- , PbO_3^- , PbO_2H_2^- , PbO_2H^- , PbO_2^- , PbOH_2^- , PbOH^- , PbO^- , Pb^- , H_2O^- , OH^- , O^- ion species obtained from sample E; they are very important in the evaluation of film activity and their in depth profiles have been performed for a more complete characterization. In Figs. 5(a)–5(d), respectively, the 17/16, 18/16, 18/17, and 19/16 negative ion profile ratios obtained during 14 min of O_2^+ primary ion bombardment are reported. The curve shapes confirm the in-depth presence of H_2O and hydroxyl species, the surface and near-surface presence of fluorine as impurities and a significant enrichment of OH^- species on the surface region.

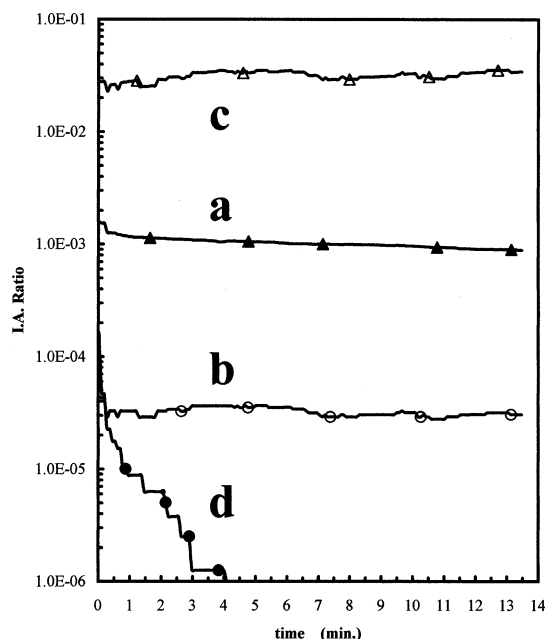


Fig. 5. Negative ion depth profile ratios for sample from group E. (a) 17/16; (b) 18/16; (c) 18/17; (d) 19/16.

Figs. 4(b) and 6(a)–6(d) show the results originated from sample F and the new species PbO_2^2H^- , $^2\text{HO}^-$, OH^2H^- , $^2\text{H}_2\text{O}^-$ have to be considered. Again, the in-depth presence of water is evident. Particularly the $^2\text{HO}^-/\text{O}^-$ (18/16, b) profile ratio exhibits a nearly constant distribution and both OH^-/O^- (17/16, a) and $^2\text{HO}^-/\text{O}^-$ profile ratios confirm the surface presence of H_2O . The $(\text{F}^- + \text{H}^2\text{HO}^-)/\text{O}^-$ (19/16, d) profile ratio shows F^- contamination in the outer layers [see Fig. 4(b)] and constant values in the inner layers than can be attributed to the H^2HO^- species.

The prolonged dipping of samples G in H_2O containing $\text{Pb}(\text{NO}_3)_2 + \text{HNO}_3$ favors H_2O penetration but real exchange with $^2\text{H}_2\text{O}$ is not immediately evident. In Fig. 4(c), higher ion yields of $m/z = 20$, 19, 18, 17 principally attributed to $^2\text{H}_2\text{O}^-$, $(\text{H}^2\text{HO}^- + \text{F}^-)$, $(^2\text{HO}^- + \text{H}_2\text{O}^-)$, OH^- species can be observed and analogously lead-related peaks show high relative intensity; other than the PbO_xH_y^- species, PbO_2^2H^- , $\text{PbO}_2\text{H}^2\text{H}^-$, PbO^2H^- are also present. The “new” matrix also reveals a higher presence of CH_n^- , C_2H_n^- species and their reactivity with PbO_2 films produce PbC^- , PbC_2^- , PbC_2O^- species.

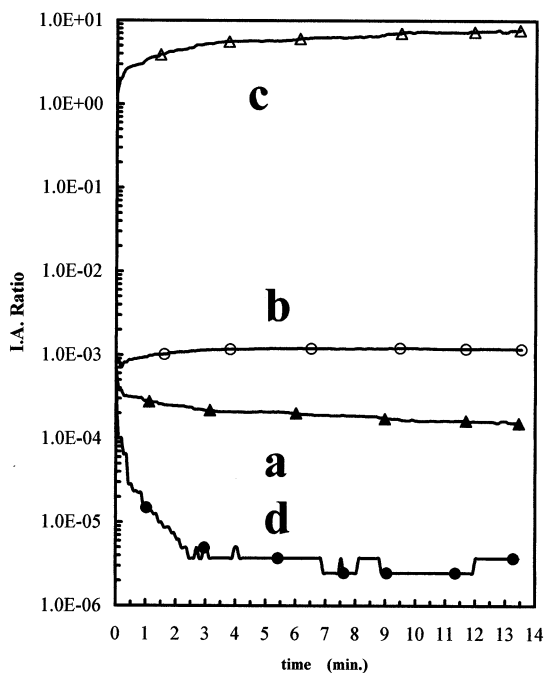


Fig. 6. Negative ion depth profile ratios for sample from group F. (a) 17/16; (b) 18/16; (c) 18/17; (d) 19/16.

Figs. 7(a)–7(d) report on profile ratios confirming the penetration in the film of H_2O , $^2\text{H}_2\text{O}$, H_2O surface enrichment and minor interference of F^- ions at $m/z = 19$. Furthermore, a comparison of Figs. 5, 6, and 7 suggests that as expected, the OH^-/O^- profile ratio of H_2O -prepared samples E maintains values higher than that of $^2\text{H}_2\text{O}$ -prepared samples F; the highest values obtained for samples G confirm a more significant presence of H_2O ; this is also in agreement with the data relative to the 18/16, 19/16, 18/17 profile ratios; analogous considerations explain the lower values of the 18/16 profile ratios for samples E; the presence of the $^2\text{HO}^-$ fragment increases the $m/z = 18$ signal which is linearly correlated to $^2\text{H}_2\text{O}$.

4. Conclusions

New experiments based on SIMS and radiochemical methodologies have confirmed the water content on the surface and into the bulk of Pb oxide films. The water amount and its distribution along the thickness

affect the presence and the ionic yield of analyzed species. In particular, the electrochemical synthesis procedures (acid or alkaline bath) accomplish the codeposition of various fragments that differentiate in particular the related ion mass spectra. In fact, basic electrolytes induce heterometal cluster-rich spectra, whereas on the contrary, the acid ones show these ionic signals with very low intensity.

Furthermore, species distribution, mainly referred to alkali metals, hydroxide, and water, was influenced by aging, heating, and electrochemical treatments, causing noticeable changing in ionic mass spectra and depth profiles.

Based on these results, SIMS appears to be a particularly suitable method for the clarification of the different effects of the various treatments and synthesis procedures for PbO_2 materials. Consequently, future experiments will be carried out with the aim of studying Pb oxide structural modifications induced by dopant addition to electrochemical baths.

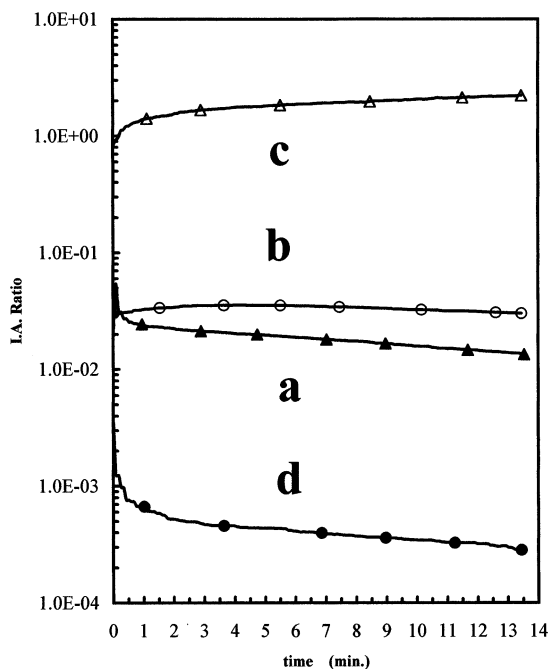


Fig. 7. Negative ion depth profile ratios for sample from group G. (a) 17/16; (b) 18/16; (c) 18/17; (d) 19/16.

Acknowledgement

Progetto Finalizzato “Materiali Speciali per Tecnologie Avanzate II,” funded by CNR, provided financial assistance for this work.

References

- [1] P. Ruetschi, R. Giovanoli, *Power Sources* 13 (1991) 81.
- [2] P. Ruetschi, *J. Electrochem. Soc.* 139 (1992) 1347.
- [3] K.D. Naegele, W.J. Plieth, *Electrochim. Acta* 25 (1980) 241.
- [4] S.M. Caulder, J.S. Murday, A.C. Simon, *J. Electrochem. Soc.* 120 (1973) 1515.
- [5] K.S. Kim T.J. O’Leary, N. Winograd, *Anal. Chem.* 45 (1973) 214.
- [6] P.T. Moseley, J.L. Hutchison, M.A.M. Bourke, *J. Electrochem. Soc.* 129 (1982) 876.
- [7] J.D. Jorgensen, R. Varma, F.J. Rotella, G. Cook, N.P. Yao, *J. Electrochem. Soc.* 129 (1982) 1678.
- [8] P.T. Moseley, J.L. Hutchison, C.J. Wright, M.A.M. Bourke, R.I. Hill, V.S. Rainey, *J. Electrochem. Soc.* 130 (1983) 829.
- [9] A. Santoro, P. d’Antonio, S.M. Caulder, *J. Electrochem. Soc.* 130 (1983) 1451.
- [10] P. Boher, P. Garnier, J.R. Gavarri, *J. Solid State Chem.* 52 (1984) 146.
- [11] P. Boher, P. Garnier, J.R. Gavarri, *J. Solid State Chem.* 55 (1984) 54.
- [12] J.P. Pohl, Schlechtriemen, *J. Appl. Electrochem.* 14 (1984) 521.
- [13] R.J. Hill, M.R. Houchin, *Electrochim. Acta* 30 (1985) 559.
- [14] P.C. Foller, C.W. Tobias, *J. Phys. Chem.* 85 (1981) 3238.
- [15] S. Daolio, B. Facchin, C. Pagura, A. De Battisti, S. Gelosi, *Inorg. Chim. Acta* 235 (1995) 381.
- [16] S. Gelosi B. Facchin, M. Fabrizio, C. Piccirillo, A. De Battisti, L. Nanni, *Syntheses and Methodologies in Inorganic Chemistry*, S. Daolio, E. Tondello, P.A. Vigato (Eds.), Vol. 7, p. 252 (1997).
- [17] R. Amadelli, A.B. Velichenko, E. Tondello, S. Daolio, M. Fabrizio, S. Gelosi, *Ossidi semplici e misti come materiali innovativi*, Torino, June 22–25, 1997. Proceedings, CP 23.
- [18] P. Ruetschi, R.T. Angstadt, B.D. Cahan, *J. Electrochem. Soc.* 106 (1959) 547.
- [19] C. Pagura, S. Daolio, B. Facchin, *Secondary Ion Mass Spectrometry SIMS VIII*, A. Benninghoven, K.T.F. Jansen, J. Tumpner, H.W. Werner (Eds.), Wiley, Chichester, 1992, p. 239.